University of Nebraska - Lincoln

DigitalCommons@University of Nebraska - Lincoln

8-2010

Unique Functionality of 22 nt miRNAs in Triggering RDR6-Dependent siRNA Biogenesis from Target Transcripts in Arabidopsis

Josh T. Cuperus
Oregon State University

Alberto Carbonell
Oregon State University

Noah Fahlgren
Oregon State University, NFahlgren@danforthcenter.org

Hernan Garcia-Ruiz
Oregon State University, hgarciaruiz2@unl.edu

Russell T. Burke
Oregon State University

See next page for additional authors

Authors

Josh T. Cuperus, Alberto Carbonell, Noah Fahlgren, Hernan Garcia-Ruiz, Russell T. Burke, Atsushi Takeda, Christopher M. Sullivan, Sunny D. Gilbert, Taiowa A. Montgomery, and James C. Carrington

Unique Functionality of 22 nt miRNAs in Triggering RDR6-Dependent siRNA Biogenesis from Target Transcripts in Arabidopsis

Josh T. Cuperus[1,2,6], **Alberto Carbonell**[2,6], **Noah Fahlgren**[1,2], **Hernan Garcia-Ruiz**[2], **Russell T. Burke**[2], **Atsushi Takeda**[4], **Christopher M. Sullivan**[2,3], **Sunny D. Gilbert**[2,3], **Taiowa A. Montgomery**[1,5], and **James C. Carrington**[2,3]

[1]Molecular and Cellular Biology Program, Oregon State University, Corvallis, OR 97331

[2]Department of Botany and Plant Pathology, Oregon State University, Corvallis, OR 97331

[3]Center for Genome Research and Biocomputing, Oregon State University, Corvallis, OR 97331

Abstract

RNA interference pathways may involve amplification of secondary siRNAs by RNA-dependent RNA polymerases. In plants, RDR6-dependent secondary siRNAs arise from transcripts targeted by some microRNA (miRNA). Here, *Arabidopsis thaliana* secondary siRNA from mRNA, and trans-acting siRNA, are shown to be triggered through initial targeting by 22 nt miRNA that associate with AGO1. In contrast to canonical 21 nt miRNA, 22 nt miRNA primarily arise from foldback precursors containing asymmetric bulges. Using artificial miRNA constructs, conversion of asymmetric foldbacks to symmetric foldbacks resulted in production of 21 nt forms of miR173, miR472 and miR828. Both 21 and 22 nt forms associated with AGO1 and guided accurate slicer activity, but only 22 nt miRNA were competent to trigger RDR6-dependent siRNA from target RNA. These data suggest that AGO1 functions differentially with 21 and 22 nt miRNA to engage the RDR6-associated amplification apparatus.

INTRODUCTION

During RNA interference (RNAi), double stranded RNA (dsRNA) is processed by Dicer, a dsRNA-specific RNase III class ribonuclease, into small ~20–30 nt RNA duplexes. Typically, one strand of the duplex preferentially associates with an Argonaute protein to form an effector complex (RNA-induced silencing complex, or RISC), that targets and silences transcripts based on sequence complementarity[1]. In plants, fungi, nematodes, and some other organisms, this process can be amplified through production of secondary short interfering RNAs (siRNAs) after transcription by RNA-dependent RNA polymerase (RdRp) on the primary target RNA[2]. As exemplified in *Caenorhabditis elegans*, primary siRNA, secondary siRNA and other small RNA may serve as guides in association with distinct Argonaute proteins[3–5]. Additionally, dsRNA precursors or siRNA have the potential to act non-cell-autonomously in plants and some animals, leading to spread of silencing signals, subsequent amplification, and transgenerational silencing in some cases[2,6].

In amplification-competent organisms, the selective recruitment and activity of RdRp on primary targets is a key step that governs whether or not secondary siRNA and amplification occurs. The partially redundant RdRps RRF-1 and EGO-1 from *C. elegans*, QDE-1 from *Neurospora crassa*, Rdp1 from *Schizosaccharomyces pombe*, and RNA-DEPENDENT RNA POLYMERASE6 (RDR6) from *Arabidopsis thaliana* transcribe RNA in a primer-independent manner[7–12]. *A. thaliana* may encode six RdRps, at least three of which generate long dsRNA that serve as DICER-LIKE (DCL) substrates in several distinct pathways[2,13]. RDR6, which frequently functions in combination with DCL4, participates in posttranscriptional silencing of exogenous targets (transgene transcripts, some viral RNA), as well as several types of endogenous transcripts[13,14]. Indiscriminant entry of transcripts into the RDR6-dependent siRNA amplification pathway does not occur in plants. Amplification of secondary siRNA occurs, however, from a minority of small RNA-targeted transcripts, and the genetic requirements for biogenesis of these siRNA resemble those of trans-acting siRNA (tasiRNA)[15–20]. Tightly controlled entry of transcripts into amplification pathways makes intuitive sense, as feed-forward amplification of silencing signals could conceivably result in runaway suppression of off-target transcripts from related gene family members. In Arabidopsis, the XRN family of exonucleases functions to degrade sliced transcript fragments[21], and sequencing analysis using an *xrn4* mutant suggests that XRN4 is antagonistic to secondary siRNA biogenesis[22]. How secondary siRNA-producing transcripts are routed differentially from most other target transcripts is understood poorly.

Plant tasiRNA represent a case in which an RdRp-dependent, secondary siRNA-producing pathway has evolved to produce specialized small RNA that function to repress co-evolved targets. The four known families of tasiRNA (*TAS1-TAS4*) in Arabidopsis are particularly informative as experimental systems to understand formation of secondary siRNA. tasiRNAs form from primary *TAS* transcripts that are initially targeted and sliced by AGO1-miR173 (*TAS1, TAS2*), AGO1-miR828 (*TAS4*) or AGO7-miR390 (*TAS3*) complexes[18,23–26]. *TAS1*, *TAS2* and *TAS4* tasiRNA-generating transcripts are cleaved at a 5'-proximal site. The 3' RNA product is then transcribed by RDR6, leading to dsRNA that is sequentially processed by DCL4 to yield phased tasiRNA in register with the cleavage site[18,23,26–30].

Here, the basis for selective entry of miRNA-targeted transcripts through the RDR6-dependent siRNA-generating pathway was investigated. Combining genome-wide analyses of 21 nt siRNA and miRNA-targeting patterns with directed experiments, miRNA length was found to be a key determinant in triggering amplification in the context of AGO1-miRNA complexes. In addition, determinants within *MIRNA* foldbacks that govern miRNA size were identified.

RESULTS

Secondary siRNAs originate from some targeted mRNAs

Six *A. thaliana* small RNA libraries were generated from aerial plant tissue and sequenced in a multiplexed format, yielding an average of 658,999 reads/library that mapped to at least one genomic position. Among 20–24 nt reads, 53.9% were 21 nts, the vast majority of which corresponded to miRNA (Supplementary Fig. 1). A significant proportion of 20–24 nt reads (74.4%) mapped to 979 annotated transcripts, 55 of which are known to be targeted by one or more miRNA or tasiRNA (Fig. 1a, Supplementary Table 1). Although targeted transcripts represented only 5.6% of the 979 small RNA-generating transcripts, reads from the targeted set represented 27.0% of reads from the entire transcript set. Among reads mapping to the targeted transcripts, 85.4% were 21 nt in length, whereas the majority (52.9%) of reads derived from non-targeted transcripts were 24 nts in length (Fig. 1a,b). Twenty-one-nucleotide siRNA originating from the targeted transcripts were shown previously to be largely RDR6- and DCL4-dependent[15]. Thus, among Arabidopsis siRNA originating from annotated transcripts, those from targeted transcripts are more likely to yield siRNA of 21 nts in length.

A total of 280 miRNA-target or tasiRNA-target pairs were collated from published data (Supplementary Table 2). Given that multigene families with many members targeted by a specific miRNA or tasiRNA family tend to bias representation on this list, "non-redundant" sets of miRNA-target and tasiRNA-target pairs were generated. One hundred non-redundant set iterations (50 pairs in each) contained only one paralog/target family/small RNA, with the targeted family member chosen randomly for each family in each iteration. Most targeted transcripts from the non-redundant list yielded no 21 nt siRNA (Fig. 1c, Supplementary Table 2). However, on average 33.8% of targets yielded at least a few siRNAs, with several targets yielding highly abundant 21 nt siRNA (Fig. 1c). Levels of these abundant siRNAs were decreased in the *dcl2-1 dcl3-1 dcl4-2* (termed *dcl234*) triple mutant (Fig. 1c).

In exploring the differences between small RNA-target pairs that led to secondary siRNA production and those that did not, it was noticed that secondary siRNA-generating transcripts were frequently targeted by miRNA or tasiRNA of 22 nts in length (Fig. 1d). Targets that interacted with miRNA or tasiRNA containing less than 22 nts yielded significantly (*p*=0.034, permutation test) less siRNA on average. Additionally, 47% of singly targeted transcripts and 43% of multiply targeted transcripts presented in Figure 1a were targeted by a small RNA of predominantly 22 nts in length. The biogenesis and activity of 22 nt miRNAs were therefore subjected to further analysis.

Asymmetric *MIRNA* foldbacks yield 22 nt miRNA

The vast majority of Arabidopsis miRNA reads were either 21 or 22 nts in length, with 22 nt families representing 22.5% of all annotated *MIRNA* families (Fig. 2a). The overall abundance of 22 nt miRNA reads, however, was relatively low (2.3%). Both the percentage of 22 nt-generating *MIRNA* families, and the numbers of 22 nt miRNA reads, were comparably low in rice (Fig. 2a; Supplementary Table 3,4). Size was also a distinct characteristic for most *MIRNA* families in both Arabidopsis and rice, with relatively few families expressing a mixed size distribution. Comparing the proportions of 21 or 22 nt miRNA from non-redundant loci in Arabidopsis and rice revealed a distinct bimodal distribution; over 90% of all *MIRNA* loci generated miRNA that were >80% either 21 nt or 22 nt in length (Fig. 2b; Supplementary Table 3,4). To understand the basis for 21 vs. 22 nt miRNA formation, foldback base-pairing patterns of Arabidopsis *MIRNA* were examined. Strikingly, those Arabidopsis foldbacks that contained asymmetry in the form of a non-paired nucleotide within the miRNA sequence were significantly enriched for 22 nt miRNA reads ($p < 2.6\ 10^{-9}$, Wilcoxon rank sum test) (Fig. 2c). In nearly all cases of predominantly 22 nt miRNA, including miR173, miR393 and miR472, an asymmetric non-paired base was detected; there were a few exceptions, such as miR828, which arose from a foldback containing only symmetric mispairs within the miRNA/miRNA* segment (Fig. 2d, Supplementary Table 3).

To determine if the asymmetric positions within miRNA sequences of foldbacks led to formation of the 22 nt size miRNA, artificial miRNA (amiRNA) were expressed using foldbacks containing either asymmetric (wild-type configuration) or symmetric miRNA/ miRNA* segments. These were produced using the *MIR390a* foldback, in which the miR390/miR390* sequences were replaced by miR173/miR173* sequences[25]. The symmetric foldback was engineered by the addition of a U residue to base-pair with the normally mispaired A residue within the *MIR173* foldback (Fig. 3a). The authentic *MIR173* foldback, and the asymmetric and symmetric amiRNA foldbacks, were coexpressed with the tasiRNA-generating construct, *35S:TAS1c*, in transient assays using *Nicotiana benthamiana*[23], and both miRNA and tasiRNA accumulation (see below) were measured in blot assays and by sequence analysis. Neither miR173 nor *TAS1c* tasiRNA are conserved in *Nicotiana* species, so accumulation of these small RNAs is entirely dependent on the transient expression assay. The asymmetric foldback, from either the authentic (*35S:MIR173*) or artificial (*35S:amiR173*) constructs, yielded predominantly 22 nt-size miR173 in blot assays (Fig. 3b). In contrast, the symmetric foldback (*35S:amiR173-21*) yielded a 21 nt-size miR173 (Fig. 3b). Sequence analysis of small RNAs from these assays confirmed that the asymmetric foldbacks yielded predominantly 22 nt miR173, although a substantial amount of off-size products of 19 and 20 nts were sequenced (Fig. 3c, Supplementary Fig. 2, Supplementary Table 5). The symmetric foldback, however, yielded miR173 that was 91% 21 nt in length (Fig. 3c, Supplementary Fig. 2, Supplementary Table 5). The 21 nt form lacked the 3'C residue present in authentic miR173.

Several previous reports collectively showed that miR173 formation requires DCL1, but not DCL2[30]–[32]. DCL2, however, was shown to produce 22 nt siRNA from endogenous Arabidopsis dsRNA[27],[29]. To determine if DCL2, or siRNA-generating DCL3 and DCL4,

are necessary for 22 nt miRNA, miRNA reads sequenced from Col-0 and the *dcl234* triple mutant were compared. Accumulation and family representation levels of most miRNAs in the *dcl234* triple mutant, regardless of size, were similar to those in wild-type Col-0 plants (Fig. 2a, Supplementary Fig. 3a,b). miRNA reads from Col-0 and *dcl234* mutant plants for most families, except for two (miR822 and miR839, which are known to be DCL4-dependent[18]), were highly correlated (Pearson product-moment correlation coefficient [r] = 0.95) (Supplementary Fig. 3b). A high correlation (r = 0.94) was shown when only 22 nt miRNA reads were compared (Supplementary Fig. 3b). Therefore, all known 22 nt miRNA in Arabidopsis are likely DCL1-dependent.

22 nt forms of miR173, miR472, and miR828 trigger siRNAs

As shown previously[23],[30] and in Figure 3b, coexpression of *35S:MIR173* with *35S:TAS1c* triggered tasiRNA biogenesis. Authentic-size miR173 generated from *35S:amiR173* also triggered *TAS1c* tasiRNA formation (Fig. 3b, **lane 5**). The tasiRNA pools triggered by both 22 nt miR173 sources were highly phased, with the register set by the miR173 cleavage site (Fig. 3c, Supplementary Fig. 2, Supplementary Table 6). The 21 nt form produced from the amiR173-21 foldback, however, possessed very low tasiRNA trigger activity, and the few *TAS1c*-derived siRNA that were produced exhibited no phasing pattern (Fig. 3b, c; Supplementary Fig. 2; Supplementary Table 6).

The lack of tasiRNA-trigger activity of miR173-21 could be due to one or more reasons, including failure to associate with AGO1, failure to interact with and guide cleavage of the *TAS1c* primary transcript, or loss of post-cleavage functions necessary to recruit RDR6 to the precursor transcript. Mi et al. showed that, among AGO1, AGO2, AGO4 and AGO5, miR173 associated most commonly with AGO1. To confirm that both 21 and 22 nt forms of miR173 associated with AGO1, *TAS1c* biogenesis assays in *N. benthamiana* were done with co-expression of HA-tagged AGO1, followed by coimmunoprecipitation analysis. Both 22 and 21 nt forms of miR173 co-immunoprecipitated with HA-AGO1 (Fig. 3d, **lanes 4, 6 and 8**). *TAS1c* tasiR255, produced in the presence of 22 nt miR173, also co-immunoprecipitated with HA-AGO1 (Fig. 3d, **lanes 4 and 6**). As HA-AGO1-nonassociated controls, accumulation *TAS1c* 3'D2(−) tasiRNA, which contains an AGO1-nonpreferred 5'A, and U6 RNA were analyzed. No or very low levels of *TAS1c* 3'D2(−) tasiRNA and U6 RNA were detected in the immunoprecipitated samples (Fig. 3d), indicating that HA-AGO1 was selective. To assess more broadly whether or not AGO1 associates preferentially with 21 or 22 nt miRNA, small RNAs from total RNA (input fraction) and immunoprecipitated HA-AGO1 complexes (IP fraction) were identified by high-throughput sequencing (two replicates each). Of the miRNAs that were enriched at least 2-fold in the IP fraction, miRNA families that were predominantly 20–24 nts were recovered, suggesting that AGO1 does not include or exclude miRNA based on length (Supplementary Fig. 4). All predominantly 22 nt miRNA families that met read thresholds for inclusion in the enrichment calculation were enriched in the IP fraction. Additionally, for two predominantly 21 nt miRNAs (miR397a and miR167a,b,d) that had a >30% subpopulation of 22 nt variants (Fig. 2b), both the 21 and 22 nt variants were enriched more than 2-fold in the IP fraction (Supplementary Fig. 4).

To assess guide function of 22 and 21 nt miR173 forms, 5' RACE assays were done for each co-expression assay using primers to detect the 3' product of miR173-guided cleavage. Products were detected in all three co-expression assays, and sequencing confirmed that cleavage guided by both 22 and 21 nt miR173 forms occurred at the canonical target site (Fig. 3e,f). Furthermore, both 22 and 21 nt miR173 forms destabilized *TAS1c* full-length transcripts to very low or undetectable levels (Supplementary Fig. 5).

Because the 21 nt form derived from the *35S:amiR173-21* foldback contained a 3'A rather than a 3'C residue, as is present in 22 nt authentic miR173, the effect of 3' nucleotide identity on both 21 and 22 nt forms of miR173 was examined. First, a construct (*35S:amiR173-21-3'C*) that generated a symmetric foldback yielding a 21 nt form containing a 3'C was tested (Supplementary Fig. 5a). This 21 nt-size miR173 failed to trigger tasiRNA accumulation despite guiding accurate cleavage of the *TAS1c* transcript (Supplementary Fig. 5b,c **lane 2**). Second, to assess the possibility of a preference for a specific 3' nucleotide in a 22 nt context, 22 nt miR173 variants containing 3' G, A or U were tested. Each of the variants accumulated to within 36% of the level of 22 nt miR173 containing a natural 3'C and guided accurate cleavage of the *TAS1c* transcript (Supplementary Fig. 5b,c). Interestingly, although each of the 22 nt 3'G, 3'A and 3'U variants triggered tasiRNA accumulation, the levels of tasiRNA generated were relatively low (Supplementary Fig. 5b).

To determine if the 22 nt requirement to trigger tasiRNA is specific to miR173, 22 and 21 nt artificial miRNAs for both miR472 and miR828 were generated using the *MIR390a*-based foldback, and tested using the *TAS1c* tasiRNA transient assay system. Both asymmetric and symmetric foldbacks were engineered following the same strategy as for the miR173 variants (Fig. 4a) and co-expressed with modified *TAS1c* constructs (*35S:TAS1c-472* and *35S:TAS1c-828*) in which the normal miR173 target site was substituted with sites recognized by miR472 or miR828. Based on mobility of miR472 and miR828 forms in blot assays, 22 and 21 nt variants were generated as predicted from asymmetric and symmetric foldbacks, respectively, although the asymmetric miR828 foldback yielded a mixture of both size classes (Fig. 4b). Importantly, tasiRNA were detected only in those samples containing 22 nt variants of miR472 and miR828 (Fig. 4b). Like the miR173 size variants, both the 22 and 21 nt forms of miR472 and miR828 guided accurate cleavage of the engineered tasiRNA transcripts (Fig. 4b,c) and co-immunoprecipitated with HA-AGO1 (Fig. 4d). These data clearly show that 22 nt forms of three Arabidopsis miRNAs possess unique functionality to direct tasiRNA or secondary siRNA biogenesis.

DISCUSSION

This study associated a unique class of Arabidopsis miRNA - those that are 22 nts in length - with triggering formation of secondary, RDR6/DCL4-dependent 21 nt siRNAs from primary miRNA targets. While both 22 nt and 21 nt forms of miR173, miR472 and miR828 associated with AGO1 and guided accurate cleavage of target transcripts, advancement of target RNA fragments through the 21 nt siRNA biogenesis pathway was a unique property of the 22 nt miRNA-target RNA pairs. Previous studies provided hints that 22 nt miRNAs might be associated with secondary siRNA. Arabidopsis *MIR168b* was shown to generate both 21 and 22 nt forms of miR168[33], which targets the transcript encoding AGO1 and leads

to secondary siRNAs in a homeostatic regulatory loop[33],[34]. In rice, 22 nt miRNA target sites were identified in several abundant siRNA-generating transcripts[35], suggesting that the 22 nt property may be conserved in angiosperms.

The fact that most plant miRNAs, particularly those from the most highly expressed families, are 21 nt in length may explain why secondary siRNA from most targeted transcripts are absent or in low abundance. While the tasiRNA represent highly refined examples of functional, discrete secondary siRNAs from a non-coding RNA, it is interesting to consider potential functions for the cases in which abundant siRNAs originate from protein-coding transcripts. In at least some examples, secondary siRNA might specifically target transcripts from related family members. For gene families that are evolving or expanding rapidly, secondary targeting may suppress dosage effects. Evidence for the functionality of secondary siRNA from large multigene family transcripts has been presented[15],[36],[37].

It is proposed that 22 nt miRNA-AGO1 complexes, but not 21 nt miRNA-AGO1 complexes, mark transcripts for RDR6-dependent siRNA formation. This could involve AGO1 adopting one of two states - an amplification-trigger state and a non-trigger state. Both states would be competent to interact with and slice targets containing a suitable target site, but only the trigger state would recruit RDR6 to the de-capped (sliced) target. Previous results from experiments with a non-cleavable target of miR173 suggested that secondary siRNA formation depends on a functional cleavage site[30]. Several studies have also shown that all known tasiRNA, and many other RDR6-dependent siRNA in Arabidopsis[15],[18],[19],[23], originate preferentially adjacent to target cleavage sites. Recruitment of RDR6, therefore, may depend on target cleavage.

Conformational changes of well-characterized Argonaute proteins are known to occur upon interaction with target RNA and release of the guide 3' end from the PAZ domain[38],[39]. How a 22 nt RNA would effect an AGO1 conformation distinct from a 21 nt RNA is not immediately obvious. The proposed trigger state, however, could involve a direct interaction with RDR6 or associated factors, such as SGS3[16],[26]. To date, there are no data suggesting direct interaction between AGO1 and RDR6 or known RDR6-associated factors. Alternatively, conformationally distinct AGO1-small RNA complexes may interact differentially with GW domain proteins, which interact directly with AGO proteins as scaffolds to mediate interactions with other factors to suppress translation and promote de-adenylation[40]. Arabidopsis AGO1-specific GW proteins are not yet characterized, although AGO4 likely interacts with GW domains in an RNA PolV subunit (NRPDE1) and the transcription elongation factor SPT5L[41]–[43].

While it is clear that AGO1 exhibits a preference for small RNAs with a 5'U, which docks within a MID domain binding pocket, there are no clear structural or functional data supporting a 3' nucleotide preference for interaction with the PAZ domain. Among 22 nt miRNAs in Arabidopsis, a 3'C is most common, although this implies neither a binding preference nor particular functionality. Within a 22 nt context, a 3'C promoted siRNA-trigger function of miR173 most effectively. However, there was no strict requirement for any specific 3' nucleotide, and the 22 nt siRNA-triggers miR828 and miR393 both contain

3'A. The studies presented here do not allow quantitative comparison of the affinity of AGO1 for 21 vs. 22 nt miRNAs, or for 22 nt miRNAs with different 3' nucleotides.

The finding that 22 nt miRNA trigger RDR6-dependent secondary siRNAs leads to the question of whether or not other siRNA amplification pathways have guide RNA-specific activities to recruit RDR1 or RDR2. Signals for amplification mediated by RDR1 and RDR6 during antiviral RNAi are not known, although results presented here suggest 22 nt siRNA, working through AGO1 or other AGO proteins, might be plausible triggers. As DCL2 is known to both promote a full silencing response against several viruses[32],[44]–[47] and to generate 22 nt siRNAs[27],[29], this idea may have support. DCL2 was also shown to promote DCL4-dependent posttranscriptional silencing of several transgenes[48]. Furthermore, overproduction of DCL2-dependent 22 nt siRNA may account for the severe phenotypes of *dcl134* and *dcl14* mutant Arabidopsis plants, in which DCL2 might generate 22 nt siRNA from dsRNA that would normally be processed to 21 nt siRNA by DCL4[32].

Finally, the basis for production of either a 21 nt or a 22 nt miRNA depends on the nature of the foldback in plants. Most Arabidopsis miRNAs are formed by DCL1-mediated processing first at the loop-distal end of the foldback, then at the loop proximal end[49]–[51]. DCL1, like other Dicers, functions as a molecular ruler. For the loop-proximal cuts, DCL1 "measures" the length of helical RNA from the PAZ domain-bound end to the positions juxtaposed to the active centers[52]–[54]. For foldbacks that are symmetrically paired within the miRNA/miRNA* region, it is inferred that DCL1 measures a length equivalent to 21 base pairs in most cases. However, it is also inferred that length of an A-form helix containing a single asymmetric bulge is frequently equivalent to that of a symmetrically paired helix. Three-dimensional modeling of 21 nt- and 22 nt-generating *MIR173* foldbacks using MC-Fold and MC-Sym[55] supports this idea. The most likely models show that an unpaired nucleotide does not substantially increase the length of the miRNA/miRNA* duplex region (Supplementary Fig. 6). This explains why, when the asymmetric nucleotide occurs within the miRNA sequence, the resulting miRNA contains a non-canonical 22 nt length. Given the unique functionality of 22 nt miRNA to trigger siRNA amplification, it seems reasonable to propose that foldback structures with asymmetric positions, and that would result in 22 nt miRNA, should be under evolutionary constraints.

METHODS

Plant materials and growth conditions

N. benthamiana and *A. thaliana* plants, including the previously described *dcl2-1 dcl3-1 dcl4-2* triple mutant[47], were grown in normal greenhouse conditions with supplemental light on a 16hr light/ 8 hr dark cycle.

Transgene constructs

35S:TAS1c and *35S:MIR173a* derived constructs were generated in pMDC32 and described previously[23],[25],[30],[57]. *MIR390a*-derived artificial miRNA constructs were designed by ligating overlapping oligonucleotides into a pMDC32-derived vector containing ~200bp upstream and downstream of the *MIR390a* foldback.

Transient expression assays

Transient expression assays in *N. benthamiana* leaves were carried out as previously described[58] with *Agrobacterium tumefaciens* GV3101. Bacterial cultures were resuspended at OD_{600}=1.0. When multiple constructs were co-expressed, equal amounts of each culture were used. Plants were grown in the greenhouse after infiltration, and zones of infiltration were harvested 48 hours post-infiltration for RNA isolation.

RNA Blot assays

Total RNA from Arabidopsis and *N. benthamiana* was isolated using TRIzol reagent (Invitrogen). Two chloroform extractions were done and RNA was precipitated in an equal volume of isopropanol for 20 min. Triplicate samples from pools of *N. benthamiana* infiltrated leaves were analyzed. RNA blot assays were done as described[30]. Briefly 5 μg, 10 μg or 20 μg of total normalized RNA was resolved by denaturing polyacrylamide-gel electrophoresis for small RNA analysis, or 5 μg of total RNA was resolved by denaturing 1.5% agarose-gel electrophoresis. RNA was transferred to positively charged nitrocellulose membrane. DNA or LNA probes were end-labeled using [^{32}]ATP and Optikinase (USB). Probes were hybridized to RNA on membranes in Sigma Perfect-Hyb at 68°C (HMW blots) or 38–42°C (small RNA blots). An Instant Imager (Packard Bioscience) was used to measure blot hybridization signals.

Small RNA sequencing

Small RNA amplicons from transient assays in *N. benthamiana* were prepared as described[57],[59]. Four synthetic oligoribonucleotides were added in different amounts (Std11, 0.0001 pmol; Std6, 0.001 pmol; Std3, 0.01 pmol; Std2, 0.1 pmol) to 90 μg total RNA per sample before amplicon preparation. Sequencing-by-synthesis was done with five pmol of each amplicon using an Illumina Genome Analyzer II (GAII, www.illumina.com). Reads were parsed using the first six nucleotides of the 3' adapter (CTGTAG). Reads were normalized per million as described[59]. Read proportions were based on total reads (18–24 nts) that matched perfectly within a 29 base window surrounding the miR173 or miR173* sequences from samples containing *35S:MIR173a, 35S:amiR173* and *35S:amiR173-21*. Radar plots to display phasing from *35S:TAS1c* were generated as previously described[19],[25]. Small RNA amplicons were generated and analyzed from HA-AGO1 IP samples as described[25].

Small RNA analysis

Small RNA from *A. thaliana* were mapped to the genome and annotated transcriptome (TAIR9; http://www.arabidopsis.org), including annotated *MIRNA* precursors (miRBase v14; http://www.miRBase.org), using the CASHX pipeline[59]. Those transcripts to which four or greater small RNA reads/million (RPM) were mapped in at least four of the six libraries were defined as small RNA-generating transcripts. For analysis of small RNA-generating transcripts, annotated structural RNA, pseudogenes or transposable elements were removed.

Statistical analyses

All statistical analyses were done using R v2.9.2. Permutation tests were done using the R "twotPermutation" function, with 1 million simulations, from the DAAG package[60]. A Wilcoxon rank sum test was used to compare empirical logits for the ratio of 22 to 21 nt miRNA reads. The rank sum test was done using the R "wilcox.test" function from the stats package.

5' RACE

Modified RNA ligase-mediated 5' RACE was done as described[30] with the Generacer kit (Invitrogen) using the following gene specific primers: TAS1c_707_5'_RACE [GATGATGCTTCTTCGCTACACCTCGGAG] and TAS1c_573_5'_RACE [AGCAACTGTTCTTTAGACGACTTGAAAATCTCAT]. 5' RACE products were gel purified using Invitrogen PureLink gel extraction kit, cloned in TOPO TA (Invitrogen), introduced into *E. coli*, screened for inserts, and sequenced.

Supplementary Material

Refer to Web version on PubMed Central for supplementary material.

ACKNOWLEDGMENTS

REFERENCES

1. Kim VN, Han J, Siomi MC. Biogenesis of small RNAs in animals. Nat Rev Mol Cell Biol. 2009; 10:126–139. [PubMed: 19165215]

2. Ghildiyal M, Zamore PD. Small silencing RNAs: an expanding universe. Nat Rev Genet. 2009; 10:94–108. [PubMed: 19148191]

3. Guang S, et al. An Argonaute transports siRNAs from the cytoplasm to the nucleus. Science. 2008; 321:537–541. [PubMed: 18653886]

4. Gu W, et al. Distinct argonaute-mediated 22G-RNA pathways direct genome surveillance in the C. elegans germline. Mol Cell. 2009; 36:231–244. [PubMed: 19800275]

5. Claycomb JM, et al. The Argonaute CSR-1 and its 22G-RNA cofactors are required for holocentric chromosome segregation. Cell. 2009; 139:123–134. [PubMed: 19804758]

6. Carthew RW, Sontheimer EJ. Origins and Mechanisms of miRNAs and siRNAs. Cell. 2009; 136:642–655. [PubMed: 19239886]

7. Meister G, Tuschl T. Mechanisms of gene silencing by double-stranded RNA. Nature. 2004; 431:343–349. [PubMed: 15372041]

8. Makeyev EV, Bamford DH. Cellular RNA-dependent RNA polymerase involved in posttranscriptional gene silencing has two distinct activity modes. Mol Cell. 2002; 10:1417–1427. [PubMed: 12504016]

9. Sijen T, Steiner FA, Thijssen KL, Plasterk RH. Secondary siRNAs result from unprimed RNA synthesis and form a distinct class. Science. 2007; 315:244–247. [PubMed: 17158288]

10. Pak J, Fire A. Distinct populations of primary and secondary effectors during RNAi in C. elegans. Science. 2007; 315:241–244. [PubMed: 17124291]

11. Motamedi MR, et al. Two RNAi complexes, RITS and RDRC, physically interact and localize to noncoding centromeric RNAs. Cell. 2004; 119:789–802. [PubMed: 15607976]

12. Correa RL, Steiner FA, Berezikov E, Ketting RF. MicroRNA-directed siRNA biogenesis in Caenorhabditis elegans. PLoS Genet. 2010; 6:e1000903. [PubMed: 20386745]

13. Voinnet O. Use, tolerance and avoidance of amplified RNA silencing by plants. Trends Plant Sci. 2008; 13:317–328. [PubMed: 18565786]

14. Mallory AC, Elmayan T, Vaucheret H. MicroRNA maturation and action--the expanding roles of ARGONAUTEs. Curr Opin Plant Biol. 2008; 11:560–566. [PubMed: 18691933]

15. Howell MD, et al. Genome-wide analysis of the RNA-DEPENDENT RNA POLYMERASE6/ DICER-LIKE4 pathway in Arabidopsis reveals dependency on miRNA- and tasiRNA-directed targeting. Plant Cell. 2007; 19:926–942. [PubMed: 17400893]

16. Peragine A, Yoshikawa M, Wu G, Albrecht HL, Poethig RS. SGS3 and SGS2/SDE1/RDR6 are required for juvenile development and the production of trans-acting siRNAs in *Arabidopsis*. Genes Dev. 2004; 18:2368–2379. [PubMed: 15466488]

17. Vazquez F, et al. Endogenous trans-acting siRNAs regulate the accumulation of *Arabidopsis* mRNAs. Mol Cell. 2004; 16:69–79. [PubMed: 15469823]

18. Rajagopalan R, Vaucheret H, Trejo J, Bartel DP. A diverse and evolutionarily fluid set of microRNAs in Arabidopsis thaliana. Genes Dev. 2006; 20:3407–3425. [PubMed: 17182867]

19. Axtell MJ, Jan C, Rajagopalan R, Bartel DP. A Two-Hit Trigger for siRNA Biogenesis in Plants. Cell. 2006; 127:565–577. [PubMed: 17081978]

20. Ronemus M, Vaughn MW, Martienssen RA. MicroRNA-targeted and small interfering RNA-mediated mRNA degradation is regulated by argonaute, dicer, and RNA-dependent RNA polymerase in Arabidopsis. Plant Cell. 2006; 18:1559–1574. [PubMed: 16798886]

21. Chiba Y, Green PJ. mRNA degredation machinery in plants. J. Plant Biol. 2009; 52:114–124.

22. Gregory BD, et al. A link between RNA metabolism and silencing affecting Arabidopsis development. Dev Cell. 2008; 14:854–866. [PubMed: 18486559]

23. Allen E, Xie Z, Gustafson AM, Carrington JC. microRNA-directed phasing during trans-acting siRNA biogenesis in plants. Cell. 2005; 121:207–221. [PubMed: 15851028]

24. Baumberger N, Baulcombe DC. *Arabidopsis* ARGONAUTE1 is an RNA slicer that selectively recruits microRNAs and short interfering RNAs. Proc Natl Acad Sci USA. 2005; 102:11928–11933. [PubMed: 16081530]

25. Montgomery TA, et al. Specificity of ARGONAUTE7-miR390 interaction and dual functionality in TAS3 trans-acting siRNA formation. Cell. 2008; 133:128–141. [PubMed: 18342362]

26. Yoshikawa M, Peragine A, Park MY, Poethig RS. A pathway for the biogenesis of trans-acting siRNAs in *Arabidopsis*. Genes Dev. 2005; 19:2164–2175. [PubMed: 16131612]

27. Xie Z, Allen E, Wilken A, Carrington JC. DICER-LIKE 4 functions in trans-acting small interfering RNA biogenesis and vegetative phase change in *Arabidopsis thaliana*. Proc Natl Acad Sci USA. 2005; 102:12984–12899. [PubMed: 16129836]

28. Dunoyer P, Himber C, Voinnet O. DICER-LIKE 4 is required for RNA interference and produces the 21-nucleotide small interfering RNA component of the plant cell-to-cell silencing signal. Nat Genet. 2005; 37:1356–1360. [PubMed: 16273107]

29. Gasciolli V, Mallory AC, Bartel DP, Vaucheret H. Partially redundant functions of *Arabidopsis* DICER-like enzymes and a role for DCL4 in producing trans-acting siRNAs. Curr Biol. 2005; 15:1494–1500. [PubMed: 16040244]

30. Montgomery TA, et al. AGO1-miR173 complex initiates phased siRNA formation in plants. Proc Natl Acad Sci U S A. 2008; 105:20055–20062. [PubMed: 19066226]

31. Park W, Li J, Song R, Messing J, Chen X. CARPEL FACTORY, a Dicer homolog, and HEN1, a novel protein, act in microRNA metabolism in Arabidopsis thaliana. Curr Biol. 2002; 12:1484–1495. [PubMed: 12225663]

32. Bouche N, Lauressergues D, Gasciolli V, Vaucheret H. An antagonistic function for *Arabidopsis* DCL2 in development and a new function for DCL4 in generating viral siRNAs. EMBO J. 2006; 25:3347–3356. [PubMed: 16810317]

33. Vaucheret H. AGO1 homeostasis involves differential production of 21-nt and 22-nt miR168 species by MIR168a and MIR168b. PLoS One. 2009; 4:e6442. [PubMed: 19649244]

34. Mallory AC, Vaucheret H. ARGONAUTE 1 homeostasis invokes the coordinate action of the microRNA and siRNA pathways. EMBO Rep. 2009; 10:521–526. [PubMed: 19343050]

35. Johnson C, et al. Clusters and superclusters of phased small RNAs in the developing inflorescence of rice. Genome Res. 2009; 19:1429–1440. [PubMed: 19584097]

36. Chen HM, Li YH, Wu SH. Bioinformatic prediction and experimental validation of a microRNA-directed tandem trans-acting siRNA cascade in Arabidopsis. Proc Natl Acad Sci USA. 2007; 104:3318–3323. [PubMed: 17360645]

37. Addo-Quaye C, Eshoo TW, Bartel DP, Axtell MJ. Endogenous siRNA and miRNA targets identified by sequencing of the Arabidopsis degradome. Curr Biol. 2008; 18:758–762. [PubMed: 18472421]

38. Wang Y, et al. Structure of an argonaute silencing complex with a seed-containing guide DNA and target RNA duplex. Nature. 2008; 456:921–926. [PubMed: 19092929]

39. Wang Y, et al. Nucleation, propagation and cleavage of target RNAs in Ago silencing complexes. Nature. 2009; 461:754–761. [PubMed: 19812667]

40. Eulalio A, Tritschler F, Izaurralde E. The GW182 protein family in animal cells: new insights into domains required for miRNA-mediated gene silencing. RNA. 2009; 15:1433–1442. [PubMed: 19535464]

41. El-Shami M, et al. Reiterated WG/GW motifs form functionally and evolutionarily conserved ARGONAUTE-binding platforms in RNAi-related components. Genes Dev. 2007; 21:2539–2544. [PubMed: 17938239]

42. Bies-Etheve N, et al. RNA-directed DNA methylation requires an AGO4-interacting member of the SPT5 elongation factor family. EMBO Rep. 2009; 10:649–654. [PubMed: 19343051]

43. He XJ, et al. An effector of RNA-directed DNA methylation in arabidopsis is an ARGONAUTE 4- and RNA-binding protein. Cell. 2009; 137:498–508. [PubMed: 19410546]

44. Blevins T, et al. Four plant Dicers mediate viral small RNA biogenesis and DNA virus induced silencing. Nucleic Acids Res. 2006; 34:6233–6246. [PubMed: 17090584]

45. Deleris A, et al. Hierarchical action and inhibition of plant Dicer-like proteins in antiviral defense. Science. 2006; 313:68–71. [PubMed: 16741077]

46. Diaz-Pendon JA, Li F, Li WX, Ding SW. Suppression of antiviral silencing by cucumber mosaic virus 2b protein in Arabidopsis is associated with drastically reduced accumulation of three classes of viral small interfering RNAs. Plant Cell. 2007; 19:2053–2063. [PubMed: 17586651]

47. Garcia-Ruiz H, et al. Arabidopsis RNA-Dependent RNA Polymerases and Dicer-Like Proteins in Antiviral Defense and Small Interfering RNA Biogenesis during Turnip Mosaic Virus Infection. Plant Cell. 2010; 22:481–496. [PubMed: 20190077]

48. Mlotshwa S, et al. DICER-LIKE2 plays a primary role in transitive silencing of transgenes in Arabidopsis. PLoS One. 2008; 3:e1755. [PubMed: 18335032]

49. Mateos JL, Bologna NG, Chorostecki U, Palatnik JF. Identification of MicroRNA processing determinants by random mutagenesis of Arabidopsis MIR172a precursor. Curr Biol. 2010; 20:49–54. [PubMed: 20005105]

50. Song L, Axtell MJ, Fedoroff NV. RNA secondary structural determinants of miRNA precursor processing in Arabidopsis. Curr Biol. 2010; 20:37–41. [PubMed: 20015653]

51. Werner S, Wollmann H, Schneeberger K, Weigel D. Structure determinants for accurate processing of miR172a in Arabidopsis thaliana. Curr Biol. 2010; 20:42–48. [PubMed: 20015654]

52. Macrae IJ, et al. Structural basis for double-stranded RNA processing by Dicer. Science. 2006; 311:195–198. [PubMed: 16410517]

53. MacRae IJ, Zhou K, Doudna JA. Structural determinants of RNA recognition and cleavage by Dicer. Nat Struct Mol Biol. 2007; 14:934–940. [PubMed: 17873886]

54. Qin H, et al. Structure of the Arabidopsis thaliana DCL4 DUF283 domain reveals a noncanonical double-stranded RNA-binding fold for protein-protein interaction. RNA. 2010; 16:474–481. [PubMed: 20106953]

55. Parisien M, Major F. The MC-Fold and MC-Sym pipeline infers RNA structure from sequence data. Nature. 2008; 452:51–55. [PubMed: 18322526]

56. Meyers BC, et al. Criteria for Annotation of Plant MicroRNAs. Plant Cell. 2008; 20:3186–3190. [PubMed: 19074682]

57. Cuperus JT, et al. Identification of MIR390a precursor processing-defective mutants in Arabidopsis by direct genome sequencing. Proc Natl Acad Sci U S A. 2010; 107:466–471. [PubMed: 20018656]

58. Llave C, Xie Z, Kasschau KD, Carrington JC. Cleavage of Scarecrow-like mRNA targets directed by a class of *Arabidopsis* miRNA. Science. 2002; 297:2053–2056. [PubMed: 12242443]

59. Fahlgren N, et al. Computational and analytical framework for small RNA profiling by high-throughput sequencing. RNA. 2009; 15:992–1002. [PubMed: 19307293]

60. Maindonald, JH.; Braun, J. Data analysis and graphics using R: an example-based approach. Cambridge University Press; Cambridge; New York: 2007. p. 502
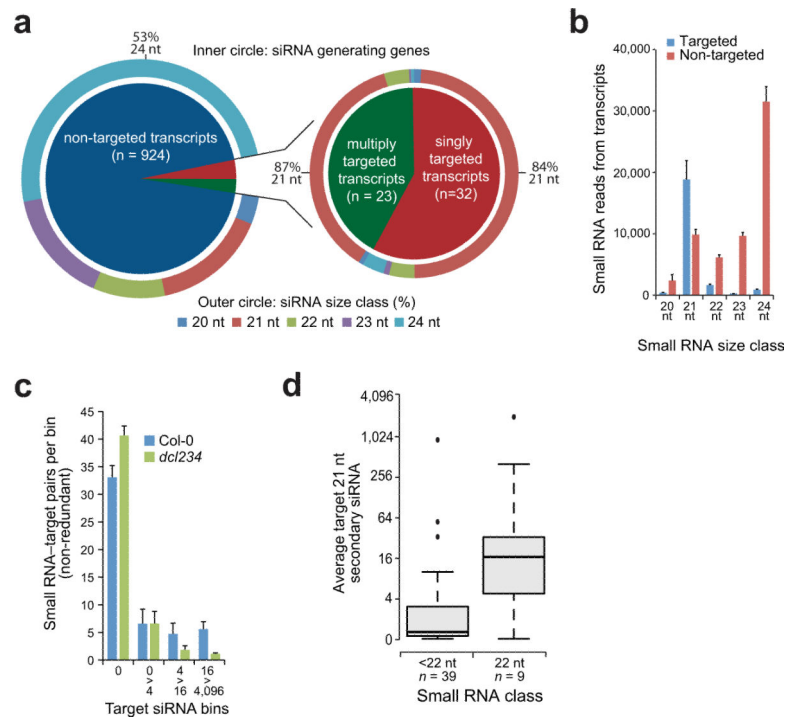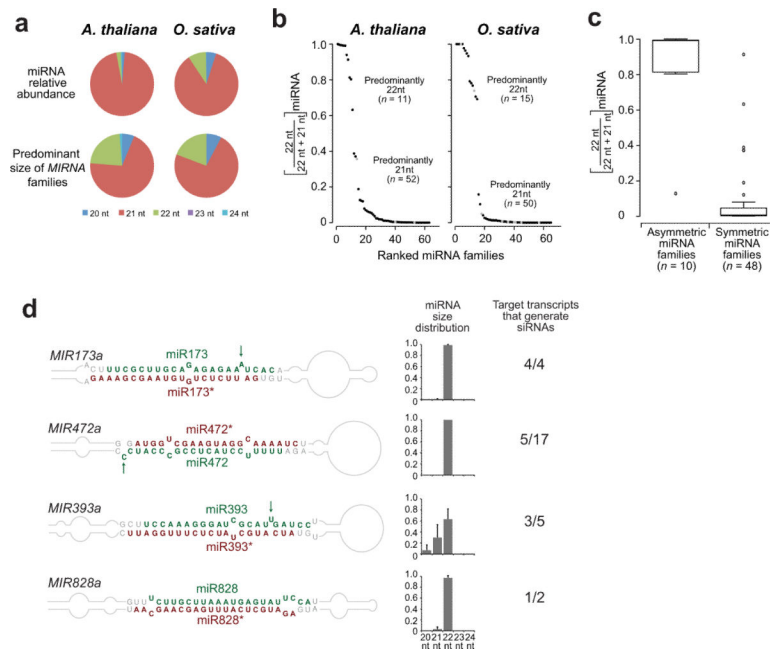
Figure 1.
Small RNA from Arabidopsis annotated transcripts. (**a**) Proportion of small RNA-generating transcripts that are targeted (at single or multiple sites) by miRNA or tasiRNA, or non-targeted. Outer rings show proportion of small RNA size. (**b**) Mean 20–24 nt siRNA levels from targeted or non-targeted transcripts. (**c**) Non-redundant small RNA-target transcript pairs yielding four levels (bins) of 21 nt siRNA in Col-0 and *dcl2-1 dcl3-1 dcl4-2* (*dcl234*) mutant plants. Data are from averages of six (Col-0) and five (*dcl234*) replicates. (**d**) Box plots showing the mean numbers of 21 nt siRNA originating from non-redundant transcripts targeted by small RNA that are 22 nt or less than 22 nt in length.

Figure 2.
MIRNA foldback asymmetry leads to formation of 22 nt miRNAs. (**a**) Mean proportions of distinct miRNA size classes in read datasets (top), and of predominant size class for MIRNA families (bottom), from Arabidopsis and rice. The rice miRNA were from a filtered subset that passed basic criteria for bona fide miRNA[56] (see Supplemental Table 4). (**b**) Rank order showing proportion of 22 nt size class, from averages of sequencing datasets, corresponding to non-redundant *MIRNA* loci in Arabidopsis and rice. Multigene *MIRNA* families with loci encoding the identical miRNA, but that have both symmetric and asymmetric foldbacks, are color coded grey. (**c**) Proportion of 22 nt miRNA from non-redundant *MIRNA* loci with base-pair asymmetry or symmetry within the miRNA/miRNA* segment of the foldback. (**d**) Examples of 22 nt miRNA-generating *MIRNA* foldbacks, average miRNA size distribution, and proportion of target transcripts that yield 21 nt siRNA (at least four reads from 4/6 replicate libraries). Green arrows indicate the predicted asymmetric position within the foldbacks.
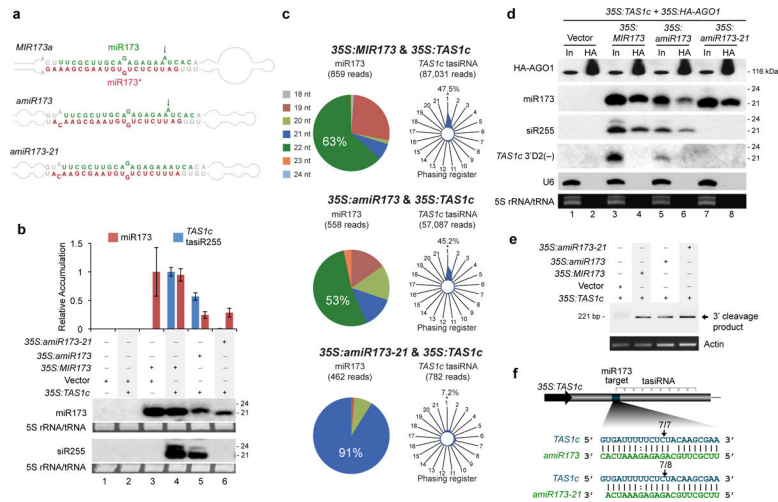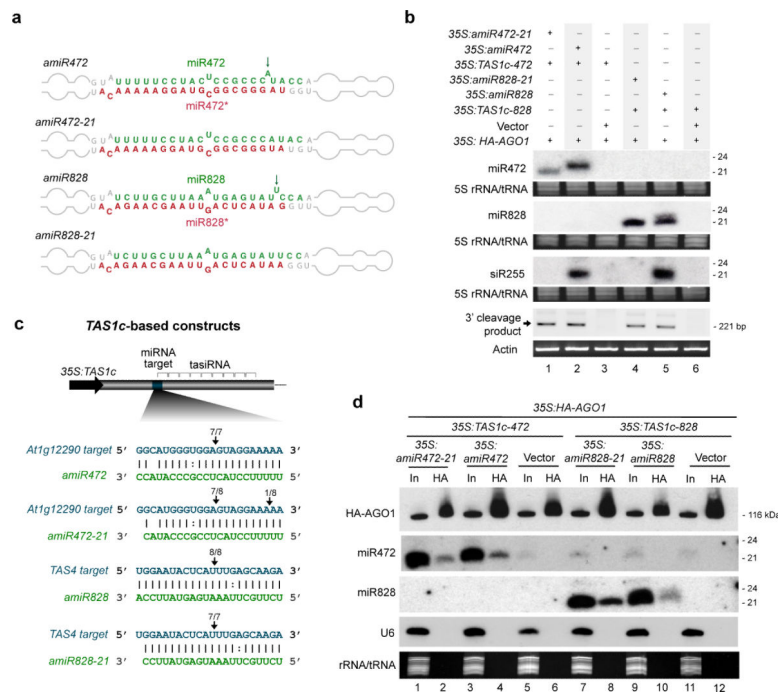
Figure 3.
Production and activities of 21 and 22 nt miR173 forms. (**a**) Foldbacks of from wild-type *MIR173, amiR173* and *amiR173-21*. Artificial miRNAs were engineered within the *MIR390a* foldback. miRNA guide and miRNA* strands are represented with green and red, respectively. The arrows indicate the predicted asymmetric position in *MIR173* and *amiR173* foldbacks. (**b**) Accumulation of miR173 and *TAS1c* tasiRNA (siR255) in *N. benthamiana* transient assays. Constructs were coexpressed as indicated above the blot panels. Mean (n=3) relative miR173 (red) and siR255 (blue) levels +/− SD (lane 2 and lane 3 = 1.0 for miR173 and tasiRNA255 respectively) were plotted (top). One of three biological replicates of the blot data, and EtBr-stained rRNA as loading controls, are shown (bottom). (**c**) Analysis of miR173 (from *35S:MIR173, 35S:amiR173* and *35S:amiR173-21*) and *TAS1c*-derived siRNA sequences by high-throughput sequencing after transient assays in *N. benthamiana*. Pie charts display the percentage of 18–24 nt reads. Radar plots display percentages of 21 nt reads corresponding to each of the 21 registers from *TAS1c* transcripts, with position 1 designated as immediately after the miR173-guided cleavage site. (**d**) Analysis of co-immunoprecipitation of 21 nt and 22 nt miR173 variants with HA-AGO1. Protein and RNA blot assays using input (in) and IP (HA) fractions from *N. benthamiana* following coexpression of *35S:HA-AGO1* and *35S:TAS1c* with *35S:MIR173, 35S:amiR173* and *35S:amiR173-21*. The *TAS1c* 3'D2(−) panel shows an HA-AGO1-nonassociated tasiRNA generated from the *TAS1c* transcript as an IP control. U6 RNA and EtBr-stained rRNA were included as input loading and HA-AGO1-nonassociated controls. (**e**) EtBr-stained 5' RACE products corresponding to the 3' cleavage product from miR173-guided cleavage. *N. benthamiana* actin RT-PCR products are shown as a control. (**f**) Proportion of cloned 5' RACE products corresponding to cleavage within *TAS1c* transcripts at the canonical miR173-guided site in assays with *amiR173* and *amiR173-21*.

Figure 4.
Production and activities of 21 and 22 nt miR472 and miR828 forms. (**a**) Foldbacks of *amiR828*, *amiR828-21*, *amiR472*, and *amiR472-21*. (**b**) Accumulation of miR472, miR828 and modified *TAS1c* tasiRNA (siR255), and 5'RACE to detect miRNA-guided cleavage products of the modified *TAS1c* transcripts, in *N. benthamiana* transient assays. (**c**) Proportion of cloned 5' RACE products corresponding to cleavage within modified *TAS1c* transcripts at the canonical miR472- or miR828-guided sites in assays with the designated artificial miRNAs. The target site sequences are actual sites from *At1g12290* and *TAS4* transcripts, which are recognized by miR472 and miR828, respectively. (**d**) Analysis of co-immunoprecipitation of 21 nt and 22 nt amiR472 and amiR828 variants with HA-AGO1. Protein and RNA assays for input (in) and IP (HA) fractions from *N. benthamiana* expressing the amiR472 and amiR828 variants were done using blots containing samples from both sets of experiments. U6 RNA and EtBr-stained rRNA were included as input loading and HA-AGO1-non-associated controls.